



## Research Article

# Machining Performance of AA2024/5Al<sub>2</sub>O<sub>3</sub>/5Gr Hybrid Composites under Al<sub>2</sub>O<sub>3</sub> Mixed Dielectric Medium

Nandagopal Kaliappan <sup>1</sup>, M. Balaji,<sup>2</sup> T. CH Anil Kumar,<sup>3</sup> Haqqani Arshad,<sup>4</sup>  
N. B. Prakash Tiruveedula,<sup>3</sup> S. Hemavathi,<sup>5</sup> and Kibebe Sahile <sup>6</sup>

<sup>1</sup>Department of Mechanical Engineering, Haramaya Institute of Technology, Haramaya University, Dire Dawa, Ethiopia

<sup>2</sup>Department of Mechanical Engineering, V R Siddhartha Engineering College, Vijayawada 520007, India

<sup>3</sup>Department of Mechanical Engineering, Vignan's Foundation for Science Technology and Research, Vadlamudi, Guntur Dt., Andhra Pradesh 522213, India

<sup>4</sup>Department of Mechanical Engineering, Yanbu Industrial Collge, Yanbu, Saudi Arabia

<sup>5</sup>Department of Battery Division, CSIR - Central Electrochemical Research Institute (CECRI), CSIR-Madras Complex, Chennai 600 113, TN, India

<sup>6</sup>Department of Chemical Engineering, College of Biological and Chemical Engineering, Addis Ababa Science and Technology University, Addis Ababa, Ethiopia

Correspondence should be addressed to Nandagopal Kaliappan; kaliappan45490@gmail.com and Kibebe Sahile; kibebe.sahile@aastu.edu.et

Received 1 January 2022; Revised 20 February 2022; Accepted 11 March 2022; Published 14 April 2022

Academic Editor: G. L. Balaji

Copyright © 2022 Nandagopal Kaliappan et al. This is an open access article distributed under the Creative Commons Attribution License, which permits unrestricted use, distribution, and reproduction in any medium, provided the original work is properly cited.

In this research work, AA2024/5Al<sub>2</sub>O<sub>3</sub>/5Gr hybrid composites fabricated through stir casting were machined utilising an electric discharge machine (EDM). Experiments were performed by varying current, pulse on time (POT), gap voltage (GV), and Al<sub>2</sub>O<sub>3</sub> powder concentration (PC). The experiments were designed using response surface methodology in which material removal rate (MRR), tool wear rate (TWR), and surface roughness ( $R_a$ ) were recorded as responses. The addition of Al<sub>2</sub>O<sub>3</sub> particles has a positive impact on MRR and  $R_a$ , whereas it has a negative impact on TWR. The interaction impact of process parameters (p-p) on responses was thoroughly analyzed using contour plots. A mathematical model was developed and validated for all the responses. The experimental results were compared with the predicted values. It was found that all the values have a maximum deviation of 3.5%. The ANOVA table reveals that the PC was the most influential factor followed by the current.

## 1. Introduction

Composites have a high strength-to-weight ratio and are the potential candidates for aerospace, marine, and defence sectors [1]. Powder metallurgy, casting, and in-situ fabrication were the distinct methods used for the fabrication of composites [2–4]. Liquid stir casting process was the most capable method for producing composites at a low cost. Attaining homogeneous distribution was the most challenging task in the manufacturing of composites [5]. In stir casting, preheated particles are mixed using a mechanical stirrer for a prescribed period of time at constant speed to achieve uniform distribution [6, 7]. Machining of

composites using conventional machining is a tedious task as the presence of hard ceramic particles causes excessive tool wear [8]. To overcome this problem, composites were machined using an unconventional machining technique. EDM, abrasive jet machining, ultrasonic machining, and electron beam machining are the distinct unconventional machining processes [9]. Of which EDM was utilized for machining harder materials with complex geometry [10].

Current, POT, pulse off time (POFT), voltage, and gap distance (GD) were the vital p-p of EDM [11]. The influence of electrical p-p on MRR, TWR, and  $R_a$  on Inconel alloy was analyzed [12]. Mineral oil with a flash point of 82C was utilized as the dielectric liquid and copper as the electrode

material. Positive polarity primes to increased MRR, whereas negative polarity precedents to lower SR values. The authors [13] etched at the effects of process factors on MRR and TWR in EDM of SKH 57 high speed steel using copper electrode material. MRR rose with  $I_p$  and peaked at approximately 100 s ton. As ton climbed, MRR decreased [14]. Current and POT are the most important factors for influencing the MRR and SR, respectively [15].

The incorporation of foreign particles improves the machining performance of EDM [16]. Boron carbide ( $B_4C$ ), silicon carbide (SiC), aluminium oxide ( $Al_2O_3$ ), and graphite (Gr) are the distinct particles incorporated in the dielectric fluid [17]. EDM of tool steel (SKH-51) with graphite nanopowder mixed dielectric was studied by [18] utilising Gr, Al, and  $Al_2O_3$  nanopowders and developed an analytical model for EDM mechanism. According to [19], boron carbide ( $B_4C$ ) powder combined with kerosene and deionized water had a significant impact on micro-performance EDM's. Tan et al. [20] investigated the machining performance of particle blended EDM and analyzed recast layer as the response. The EDM of cemented tungsten carbide utilising graphite nanopowder blended dielectric was investigated by [21]. It was reported by [22] that titanium powder combined with deionized water dielectric fluid was used to modify machined surfaces. The authors [23] investigated the impact of SiC mixed dielectric on MRR and TWR. Numerous works were reported by the researchers by adding powder particles in the dielectric fluid; however, literature linked to machining of AA2024/5 $Al_2O_3$ /5Gr hybrid composites was sparse. In this work, an attempt was made to machine AA2024/5 $Al_2O_3$ /5Gr hybrid composites by incorporating  $Al_2O_3$  particles into the dielectric fluid. The electrical process parameters altered were current, POT, and GV, in which the most influential factor was analyzed with the aid of an ANOVA table.

## 2. Materials and Methods

Aluminium alloy designated as AA2024, as procured from perfect metal alloys Bangalore, having a chemical composition as shown in Table 1, was kept in the electric furnace.

The alloy was heated to 770°C. Preheated  $Al_2O_3$  and Gr particles purchased from Bhukhanwala Industries, Mumbai, were added to the melt and stirred at a speed of 1000 rpm for 180s. The equal weight proportion of magnesium powder flux was added to the melt and, once again, the mixture was stirred for 120s. The mixture was poured into the preheated mould made of die steel. Composites of dimension (L 105 mm X ? 12 mm) were fabricated and machined to the dimension of (L 100 mm X ? 10 mm) to eliminate the surface defects. Experiments were performed on the E2K Elektra die sink EDM machine by varying current, POT, GV, and PC. The copper of dimension (L 25 mm X ? 10 mm) used as the tool material was purchased from Coimbatore Metal Mart. A new setup was laid to conduct the experiments. It comprises of dielectric tank, stirrer, pump, and motor [24] in which  $Al_2O_3$  particles of an average size of 5  $\mu$ m were added to improve the machining performance. Machining characteristics were accessed in terms of MRR, TWR, and  $R_a$ .

TABLE 1: AA2024—chemical composition.

Component	Cu	Mg	Mn	Fe	Zn	Si	Al
Wt%	4.43	1.54	0.53	0.19	0.17	0.05	Balance

Experimental runs were designed using response surface methodology in which each parameter was varied at five different levels, as shown in Table 2.

**2.1. Calculation of Response.** The MRR and TWR were calculated according to equations (1) and (2), respectively, which is the ratio of weight difference before and after machining to the machined time. The surface roughness was calculated at 5 different places using a Mitutoyo tester, and the average value was recorded. The most influential factor was analyzed using ANOVA table; a developed mathematical model was used for the computation of predicted values.

$$MRR = \left( \frac{H_b - H_a}{z} \right), \quad (1)$$

$$TWR = \left( \frac{I_b - I_a}{z} \right). \quad (2)$$

$H_b$  and  $H_a$ —sample weight before and after machining.  $I_b$  and  $I_a$ —electrode weight before and after machining.  $z$ —machined time.

## 3. Discussion of Results

**3.1. Impact of p-p on MRR.** The presence of reinforcing particles and its hard nature make it difficult for machining. The experimental results are shown in Table 3.

Materials are removed by means of melting and vaporization. The impact of various p-p on MRR is given in Figure 1. The mean MRR under pure dielectric conditions was 55.75 mg/min, but when 2.5 g of  $Al_2O_3$  particles were added to the fluid, it rose to 83.75 mg/min, and then to 87.11 mg/min when 5 g/l was added. The improvement in MRR was attributed to two factors: (1) the suspended particles get energized and move in a zig-zag fashion when the voltage is applied which facilitates the bridging effect [25].

It generates an enormous amount of heat, resulting in an improvement in MRR. (2) The addition of powder reduces the insulating strength and results in early dielectric break down [26], hence sparking occurs most frequently. With further increase in PC to 7.5 g/l, the MRR decreases. The suspended particles are packed densely inside the spark gap which hinders the machining process. The particles were not completely flushed away, resulting in the remelting of particles over the surface [27].

The MRR reduces from 101.91 mg/min to 81.16 mg/min when there is a shift in current from 7A to 16A. At 7A current, the plasma channel distributes the heat intensity uniformly over the surface [28]. With further increase in current, this plasma channel gets widened, resulting in a reduction of heat intensity, which leads to a decrease in MRR [29]. The MRR decreases until the saddle point of 45 V, thereafter it starts to reduce.

TABLE 2: Levels of EDM p-p.

P-p	Levels
PC (g/l)	0, 2.5, 5, 7.5, 10
Current (A)	7, 10, 13, 16, 19
POT ( $\mu$ s)	3, 4, 5, 6, 7
GV (V)	15, 30, 45, 60, 75
Electrode	Copper
Work piece	AA2024/5Al <sub>2</sub> O <sub>3</sub> /5Gr

TABLE 3: Experimental results and their predicted values.

S.No	Parameters				Experimental results			Predicted results		
	PC (g/l)	Current (A)	POT ( $\mu$ s)	GV (V)	MRR (mg/min)	TWR (mg/min)	Ra ( $\mu$ m)	MRR (mg/min)	TWR (mg/min)	Ra ( $\mu$ m)
1	7.5	10	4	30	98.92	18.92	4.76	98.33	19.08	4.80
2	2.5	16	4	30	72.75	21.08	4.19	72.83	20.75	4.07
3	2.5	10	4	30	88.67	20.54	3.61	89.13	21.08	3.48
4	5	13	7	45	81.42	19.21	2.78	81.88	19.50	2.86
5	5	19	5	45	91.58	20.88	2.81	92.04	21.50	2.89
6	5	13	5	45	82.29	22.29	3.28	82.43	22.29	3.28
7	10	13	5	45	54.75	26.71	8.45	55.04	26.33	8.20
8	5	7	5	45	101.92	22.04	1.86	101.88	21.17	1.94
9	7.5	16	6	30	86.42	22.58	4.88	86.83	22.42	4.93
10	5	13	5	45	83.29	22.29	3.28	82.43	22.29	3.28
11	5	13	5	45	82.29	22.29	3.28	82.43	22.29	3.28
12	2.5	10	6	30	79.58	20.42	2.86	79.67	20.25	2.74
13	5	13	5	45	82.29	22.29	3.28	82.43	22.29	3.28
14	7.5	16	6	60	80.33	24.38	5.19	79.29	24.08	5.23
15	5	13	5	15	98.58	18.04	4.24	98.88	18.17	4.33
16	5	13	5	75	94.92	20.88	4.80	95.04	20.50	4.88
17	7.5	10	6	60	72.75	23.08	4.82	72.83	23.42	4.86
18	7.5	10	4	60	87.33	22.21	5.61	87.79	22.75	5.65
19	2.5	16	6	30	83.67	19.71	5.12	82.63	19.42	5.00
20	5	13	5	45	82.29	22.29	3.28	82.43	22.29	3.28
21	5	13	3	45	87.08	20.71	2.64	87.04	20.17	2.72
22	2.5	16	6	60	88.58	18.25	4.83	89.33	18.08	4.70
23	0	13	5	45	55.75	22.21	5.94	55.88	22.33	6.35
24	7.5	16	4	60	74.92	23.75	4.30	75.00	23.92	4.35
25	7.5	16	4	30	85.00	20.71	4.50	84.79	20.75	4.54
26	5	13	5	45	82.29	22.29	3.28	82.43	22.29	3.28
27	2.5	10	6	60	86.00	19.21	3.62	85.63	19.42	3.49
28	5	13	5	45	82.29	22.29	3.28	82.43	22.29	3.28
29	2.5	16	4	60	77.67	20.88	3.40	77.29	20.92	3.27
30	7.5	10	6	30	81.33	21.04	3.47	81.13	21.25	3.51
31	2.5	10	4	60	93.08	21.58	3.86	92.83	21.75	3.73

With an increase in voltage beyond that, it accelerates the spark energy, which leads to excessive heat generation, hence more materials removed from the surface. At mean parametric value of voltage, more materials redeposit over the surface, hence MRR decreases. The POT has the very least impact on MRR; the reduction in MRR from 87.08 mg/min to 81.41 mg/min was observed when there was an increase in pulse on from 3 $\mu$ s to 7 $\mu$ s owing to the plasma expansion.

The interaction effect of various p-p on MRR is shown in Figure 2.

For the PC of 5 g/l, at 7 A current, a MRR of 101.32 mg/min was obtained. For the same parametric condition,

conventional dielectric fluid offers a MRR of 78.33 mg/min. It further reduces to 63.86 mg/min when the value of current was increased to 19 A. When 5 g/l powder for lower parametric pulse on value offers 44% lower MRR in comparison with high parametric values. The combined increase of GV and PC drastically reduces the MRR by 40%. The optimal combined parametric combination was 15 V and 5 g/l. It was clearly noted that an increase in GV, current, and POT reduces the MRR. The ANOVA Table 4 denoted that PC was the most influential factor followed by current and GV.

The maximum difference of 3.5% was observed between experimental and predicted results, and its mathematical model is shown in equation (3).

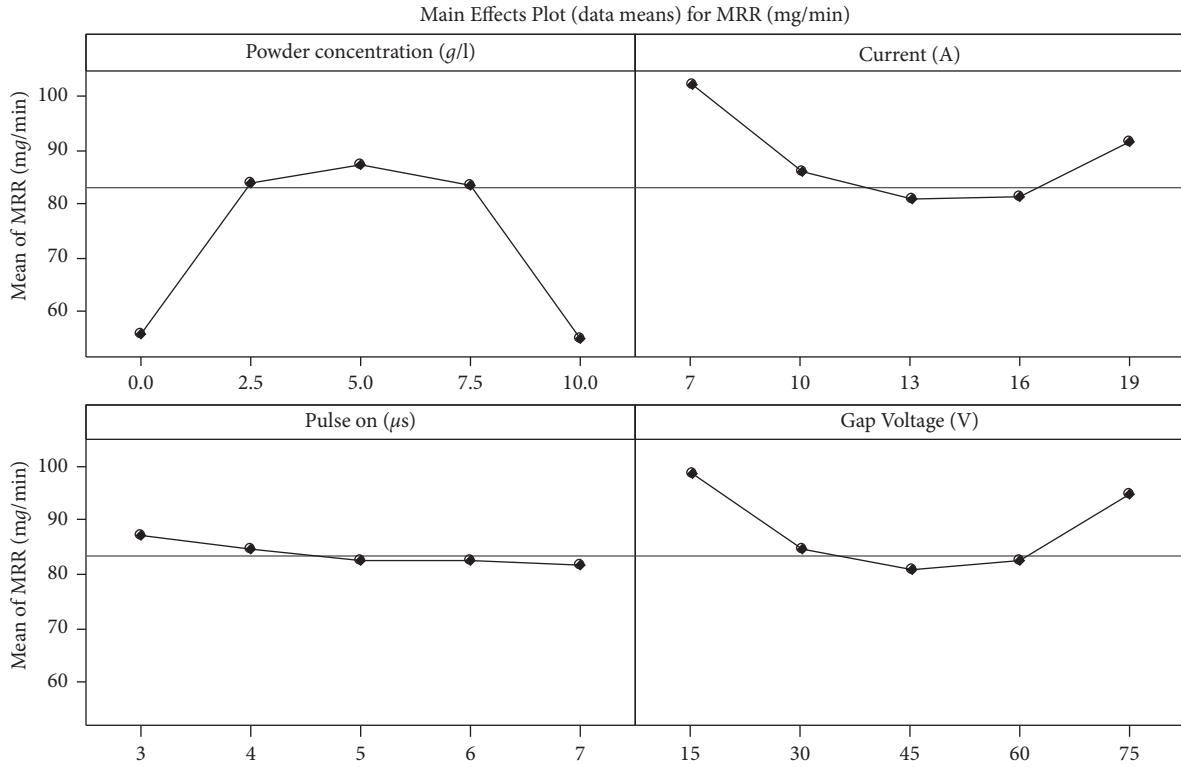


FIGURE 1: Impact of various p-p on MRR.

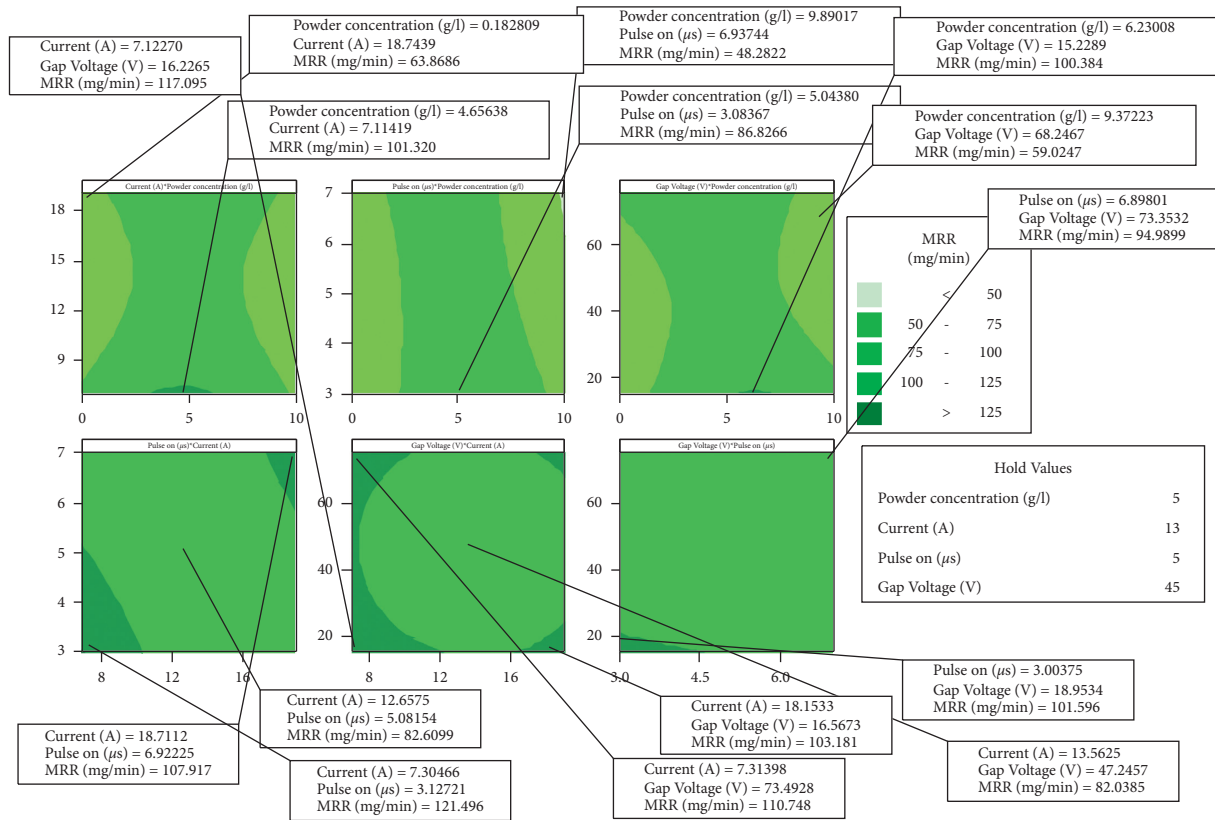


FIGURE 2: Interaction plot impact of distinct input variables vs. MRR of AA2024/5Al<sub>2</sub>O<sub>3</sub>/5Gr.

TABLE 4: Analysis of variance for MRR (mg/min).

Source	DF	Seq SS	Adj SS	Adj MS	F	P
Regression	14	3159.79	3159.79	225.699	644.03	0.000
Linear	4	208.17	208.17	52.042	148.50	0.000
Square	4	2304.75	2304.75	576.187	1644.15	0.000
Interaction	6	646.88	646.88	107.813	307.64	0.000
Residual Error	16	5.61	5.61	0.350		
Lack-of-fit	10	4.75	4.75	0.475	3.33	0.077
Pure error	6	0.86	0.86	0.143		
Total	30	3165.40				

S = 0.5920; R-Sq = 99.8%; R-Sq(adj) = 99.7%.

$$\begin{aligned}
 MRR = & 269.802 + 17.6631A - 19.9798B - 25.0327C - 1.28353 - 1.07881A^2 \\
 & + 0.403604B^2 + 0.50744C^2 + 0.0161442D^2 + 0.0916667A * B - 0.775A * C - 0.095A * D \\
 & + 1.60417B * C + 0.00416667B * D + 0.0375C * D.
 \end{aligned} \quad (3)$$

**3.2. Impact of Process Parameter on TWR.** During machining, generated heat was transferred to both the tool and the work piece. In spite of that materials were removed from the both tool and the work piece. The objective of the EDM industry was minimizing the TWR and maximizing MRR. The effect of various p-p is shown in Figure 3.

The TWR was minimum when 2.5 g/l of Al<sub>2</sub>O<sub>3</sub> were added to the dielectric fluid, and it increased with further increase in the concentration of foreign particles. When powder is added, the energized particles owing to the bridging effect reduce the spark gap. To maintain the machining condition, a slight increase in GD happened, which led to the complete dissipation of heat which reduced the TWR. At higher PC, the TWR increases owing to bridging and arcing effects [30].

With an increase in current from 7 A to 19 A, a 5% reduction in MRR was observed. It was anticipated that more heat was transferred to the work piece and also confirmed the increasing of spark gap. TWR results were diametrically opposed to MRR results in terms of GV. The minimum TWR of 18.04 mg/min was recorded at the GV of 15 V, and it was drastically increased to 22.13 mg/min at 45 V. The results confirmed that most of the heat generated was transferred to the tool material, resulting in an increase in TWR. The TWR was minimum when current was applied for the longer duration of time. At higher POT, the widening of plasma channel occurs, resulting in a reduction in TWR. The maximum difference of 4.3% was observed between experimental and

predicted results, and its mathematical model was shown in equation (4).

The interaction effect of p-p on TWR is shown in Figure 4.

Under pure dielectric medium for the 19 A current, a minimum TWR of 19.56 mg/min was obtained, and it was increased to 27.25 mg/min when the PC was increased to 10 g/l. In the case of the combinatorial effect of PC and POT, 16.92 mg/min and 27.25 mg/min TWR were recorded for the concentrations of 0 g/l and 10 g/l, respectively. With regards to POT, it offers higher TWR on low parametric value and it decreases with an increase in duration of time, irrespective of PC. Same case was reported on GV, at higher voltage, pure oil offers 17.89 mg/min and it was drastically increased to 27.55 g/min when 10 g of Al<sub>2</sub>O<sub>3</sub> was mixed in the dielectric fluid. The cumulative increase of voltage and pulse on leads to reduction in TWR; the same results were observed at lower parametric value and 20% increases in TWR was observed at intermediate value. At lower parametric values of current and POT, 16.73 mg/min were recorded and a 20% increase in TWR was observed when there was a swift change in parametric value from lower to higher. The interaction effect of pulse and current had the least impact on TWR; a minor substantial change was observed. The ANOVA Table 5 shows that PC was the most impactful factor followed by GV.

A mathematical model was developed as shown in equation (4); it showed the experimental and predicted values were well allied.

$$\begin{aligned}
 TWR = & 0.989418 - 3.68571A - 0.715608B + 6.13095C \\
 & + 0.395238 D + 0.0819048A^2 - 0.0264550B^2 - 0.613095C^2 - 0.00328042D^2 \\
 & + 0.0666667A * B + 0.300000A * C + 0.0200000A * D - 0.0416667B * C - 0.00277778B * D - 0.0250000C * D.
 \end{aligned} \quad (4)$$

**3.3. Impact of p-p on R<sub>a</sub>.** Products with a better surface finish offers the best performance along with the highest life time. The

results showed that the R<sub>a</sub> values decrease until the saddle point of 5 g/l thereafter it starts to declined, as shown in Figure 5.

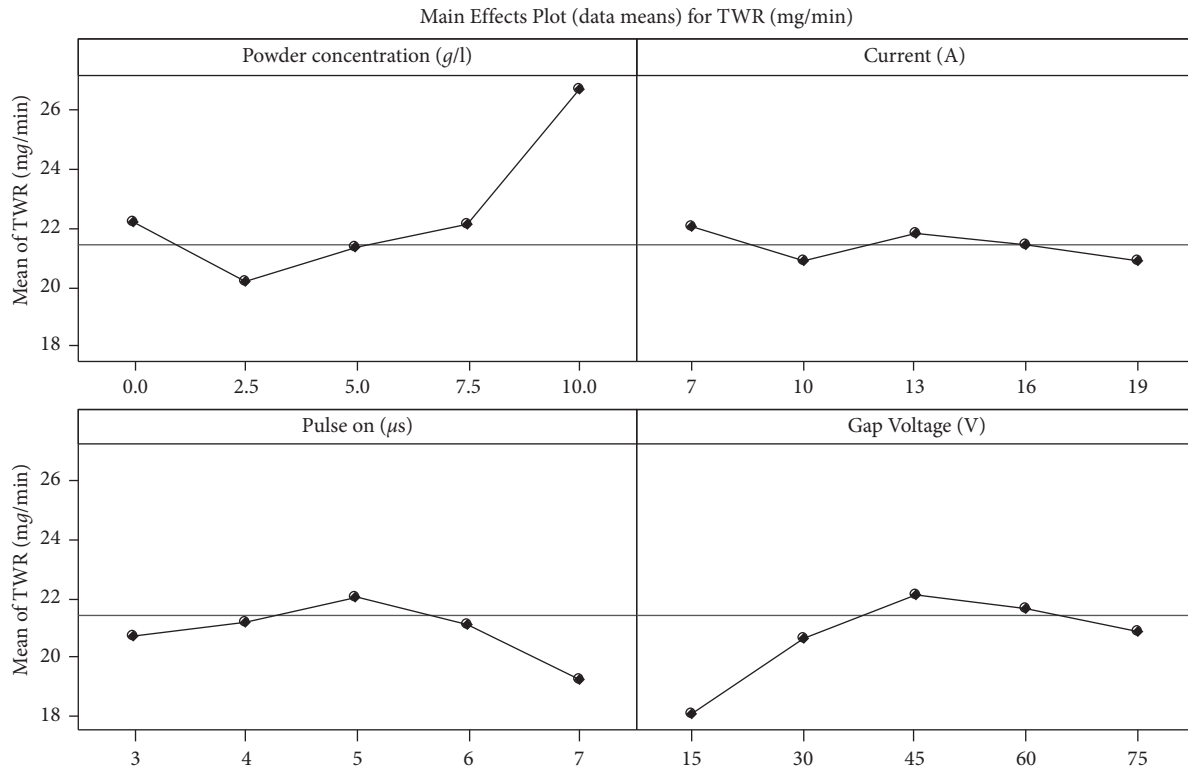


FIGURE 3: Impact of various p-p on TWR.

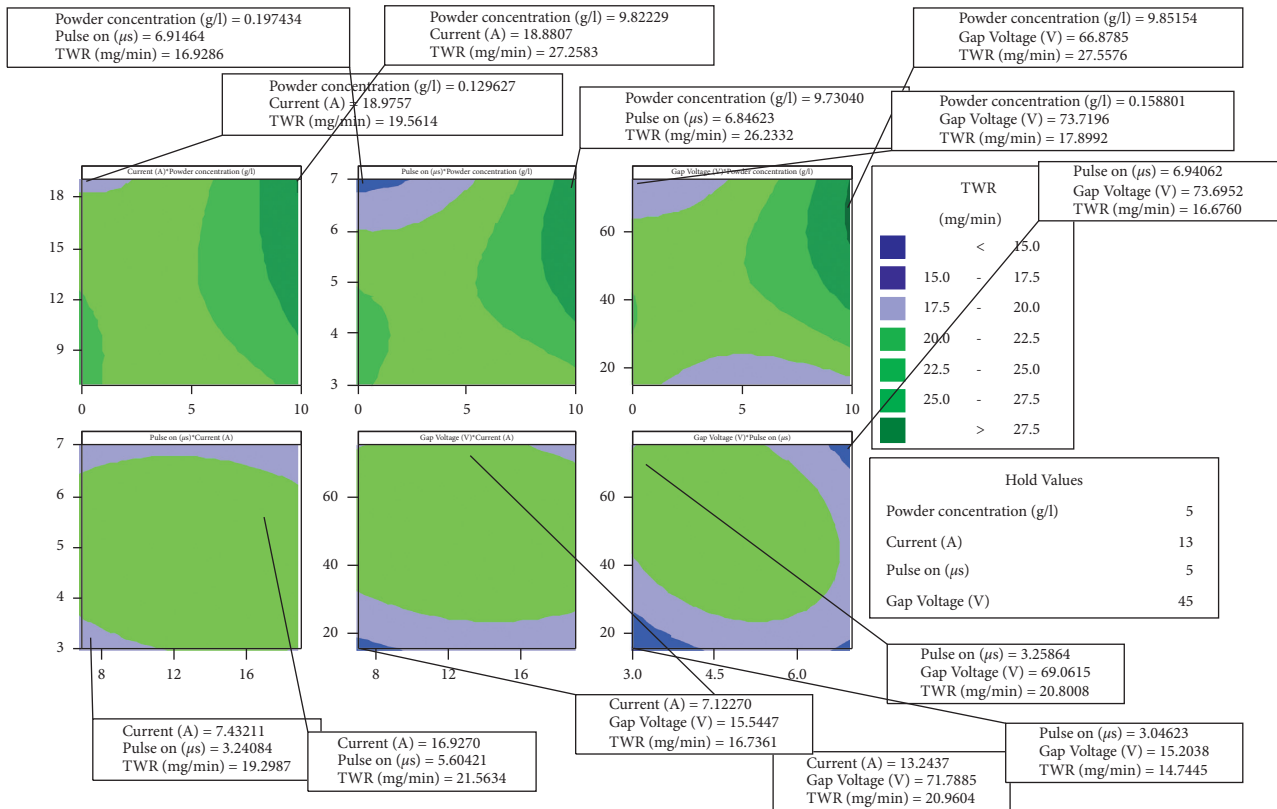
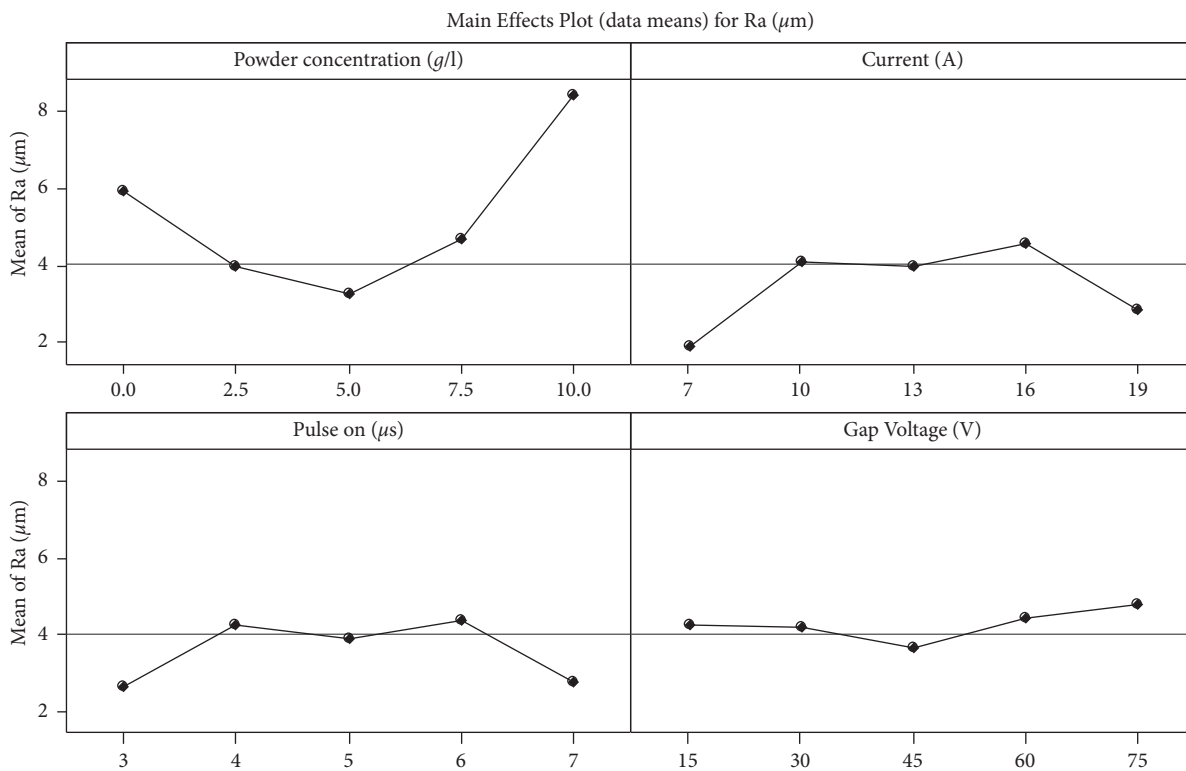


FIGURE 4: Interaction plot impact of distinct input variables vs. TWR of AA2024/5Al<sub>2</sub>O<sub>3</sub>/5Gr.

TABLE 5: ANOVA for TWR (mg/min).

Source	DF	Seq SS	Adj SS	Adj MS	F	P
Regression	14	94.4155	94.4155	6.74397	35.00	0.000
Linear	4	33.0000	33.0000	8.25000	42.81	0.000
Square	4	36.6655	36.6655	9.16638	47.57	0.000
Interaction	6	24.7500	24.7500	4.12500	21.41	0.000
Residual Error	16	3.0833	3.0833	0.19271		
Lack-of-Fit	10	3.0833	3.0833	0.30833	*	*
Pure Error	6	0.0000	0.0000	0.00000		
Total	30	97.4988				

S = 0.4390; R-Sq = 96.8%; R-Sq(adj) = 94.1%.

FIGURE 5: Impact of various p-p on  $R_a$ .

The improvement in  $R_a$  was attributed to the fact that suspension of particles increases the GD. This facilitates the complete flushing of machined debris from the spark gap [31]. It eliminates the formation of remelted layer and globules on the surface [32]. The powder particles assist in the uniform distribution of heat over the machined surface which resists the formation of craters, cracks, and pits on the surface [33]. When the powder particles weighed more than 5 g/l were added, machined debris and powder particles were densely packed inside the spark gap, resulting in incomplete flushing and leads to increase in  $R_a$  [33]. The  $R_a$  value of 1.85  $\mu\text{m}$  was observed when the parametric value of current was tuned to 7 A. Owing to its low parametric value, it generates heat of low intensity, hence  $R_a$  increases. A 15% improvement in  $R_a$  was attained when there was a reduction in GV from 15 V to 45 V. At this parametric value, most of the generated heat is transferred to the tool material which

reduces the heat intensity and hence improves surface quality. The POT, either at higher or lower parametric, yields the least  $R_a$  value. The maximum difference of 4.8% was observed between experimental and predicted results, and its mathematical model was shown in equation (5).

The combined parametric effect of p-p on  $R_a$  is shown in Figure 6.

The minimum surface roughness value of 1.79  $\mu\text{m}$  was observed when the current and PC were set at 7 A and 5 g/l respectively. Under unmixed dielectric conditions, the surface exhibited an  $R_a$  value of 6.62  $\mu\text{m}$  when the current value was tuned at 19 A. For the PC of 5 g/l, the minimum surface roughness of 2.74  $\mu\text{m}$  was attained when the POT was tweaked at 3  $\mu\text{s}$  and it was increased to 7.99  $\mu\text{m}$ , when the PC was increased to 10 g/l. The optimal  $R_a$  value of 3.22  $\mu\text{m}$  was recorded for the PC and voltage was set at 45 V and 5 g/l, respectively. The surface quality

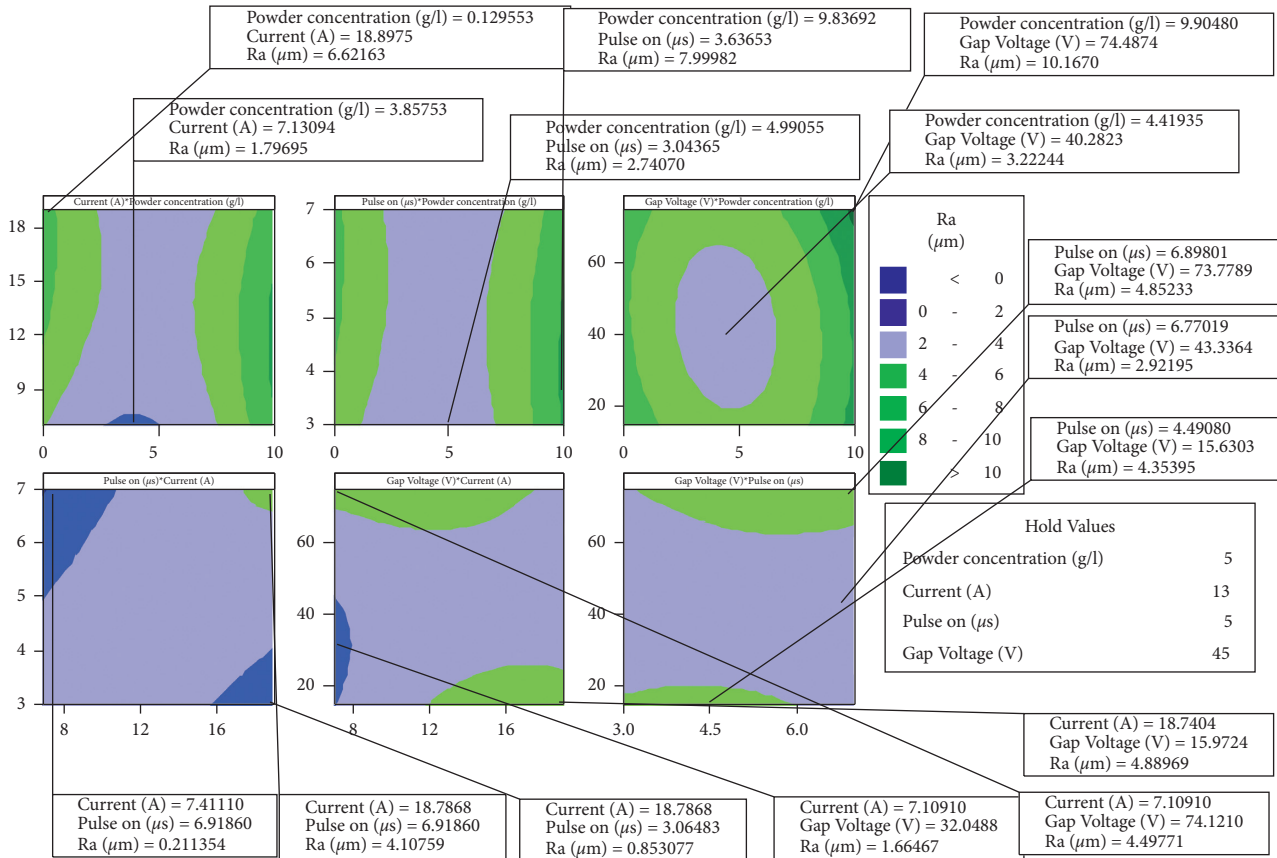


FIGURE 6: Interaction plot impact of distinct input variables vs.  $R_a$  of AA2024/5Al<sub>2</sub>O<sub>3</sub>/5Gr.

TABLE 6: Analysis of variance for  $R_a$  ( $\mu\text{m}$ ).

Source	DF	Seq SS	Adj SS	Adj MS	F	P
Regression	14	47.4269	47.4269	3.38763	130.09	0.000
Linear	4	6.9645	6.9645	1.74112	66.86	0.000
Square	4	34.9456	34.9456	8.73640	335.48	0.000
Interaction	6	5.5167	5.5167	0.91946	35.31	0.000
Residual error	16	0.4167	0.4167	0.02604		
Lack-of-fit	10	0.4167	0.4167	0.04167		
Pure error	6	0.0000	0.0000	0.00000		
Total	30	47.8435				

$S = 0.1614$ ;  $R\text{-Sq} = 99.1\%$ ;  $R\text{-Sq}(\text{adj}) = 98.4\%$ .

worsens drastically to  $10.16\mu\text{m}$  when these values are increased to  $75\text{ V}$  and  $10\text{ g/l}$ . The best surface quality was expressed when the parametric values of pulse on and voltage was set at  $45\text{ V}$  and  $7\mu\text{s}$ , respectively. Interestingly, a best surface quality of  $0.21\mu\text{m}$  was obtained for the input variables of  $7\text{ A}$  current and  $7\mu\text{s}$  POT. The most

influential factor was identified with the aid of ANOVA, as shown in Table 6.

The PC was the most impactful factor followed by the POT. The mathematical model was developed as shown in equation (5), and it was found that predicted values were well correlated with the experimental results.

$$\begin{aligned}
 R_a = & 5.92864 - 0.957912A + 0.403685B - 0.671970C \\
 & - 0.110052D + 0.160083A^2 - 0.0238452B^2 - 0.121107C^2 + 0.00147730D^2 - 0.0281333A * B \\
 & - 0.0545000A * C + 0.00399667A * D + 0.139542B * C - 0.00580556B * D + 0.00836667C * D.
 \end{aligned} \quad (5)$$



## 4. Conclusion

The AA2024/5Al<sub>2</sub>O<sub>3</sub>/5Gr hybrid composites were successfully fabricated using the stir casting technique. EDM experiments were performed on the composites by adding Al<sub>2</sub>O<sub>3</sub> in the dielectric medium, and the following findings were drawn from the studies.

- (1) Incorporation of Al<sub>2</sub>O<sub>3</sub> particles in the dielectric medium improves the MRR owing to the bridging effect and uniform heat distribution. Adding particles beyond the saddle point leads to insufficient flushing which hinders the machining process, hence MRR reduction.
- (2) Adding Al<sub>2</sub>O<sub>3</sub> particles has a negative impact on TWR. Owing to arcing and short circuits, most of the generated heat was transferred to the tool, resulting in an increase in TWR. The interaction plot reveals that current and POT have very minimal impact on TWR.
- (3) Inclusion of Al<sub>2</sub>O<sub>3</sub> particles improves the  $R_a$  of the machined surface due to the enlargement of the spark gap and complete flushing of materials. The incorporation of particles facilitates the uniform heat distribution and heat dissipation which results in the improvement of  $R_a$ .
- (4) A mathematical model was developed for all the responses, and influential factor was identified using the ANOVA table. The experimental results were compared with the predicted results, and it was found that the deviation was below 5%.

## Data Availability

The datasets used and/or analyzed during the current study are available from the corresponding author on reasonable request.

## Conflicts of Interest

There are no conflicts of interest.

## References

- [1] R. Butola, L. Tyagi, L. Kem, M. S. Ranganath, and Q. Murtaza, "Mechanical and wear properties of aluminium alloy composites: a review," *Lecture Notes on Multidisciplinary Industrial Engineering*, vol. 36, pp. 369–391, 2020.
- [2] Z. Z. Fang, J. D. Paramore, P. Sun et al., "Powder metallurgy of titanium - past, present, and future," *International Materials Reviews*, vol. 63, no. 7, pp. 407–459, 2018.
- [3] R. Ranjith, P. K. Giridharan, J. Devaraj, and V. Bharath, "Influence of titanium-coated (B<sub>4</sub>Cp + SiCp) particles on sulphide stress corrosion and wear behaviour of AA7050 hybrid composites (for MLG link)," *Journal of the Australian Ceramic Society*, vol. 53, no. 2, pp. 1017–1025, 2017.
- [4] J. Buchli, M. Giffthaler, N. Kumar et al., "Digital in situ fabrication - challenges and opportunities for robotic in situ fabrication in architecture, construction, and beyond," *Cement and Concrete Research*, vol. 112, pp. 66–75, 2018.
- [5] A. Ramanathan, P. K. Krishnan, and R. Muraliraja, "A review on the production of metal matrix composites through stir casting - furnace design, properties, challenges, and research opportunities," *Journal of Manufacturing Processes*, vol. 42, pp. 213–245, 2019.
- [6] A. Ramanathan, P. K. Krishnan, and R. Muraliraja, "A review on the production of metal matrix composites through stir casting - furnace design, properties, challenges, and research opportunities," *Journal of Manufacturing Processes*, vol. 42, pp. 213–245, 2019.
- [7] V. Mohanavel, K. S. Ashraff Ali, S. Prasath, T. Sathish, and M. Ravichandran, "Microstructural and tribological characteristics of AA6351/Si<sub>3</sub>N<sub>4</sub> composites manufactured by stir casting," *Journal of Materials Research and Technology*, vol. 9, no. 6, pp. 14662–14672, 2020.
- [8] J. Li and R. A. Laghari, "A review on machining and optimization of particle-reinforced metal matrix composites," *International Journal of Advanced Manufacturing Technology*, vol. 100, no. 9, pp. 2929–2943, 2019.
- [9] J.-P. Chen, L. Gu, and G.-J. He, "A review on conventional and nonconventional machining of SiC particle-reinforced aluminium matrix composites," *Advances in Manufacturing*, vol. 8, no. 3, pp. 279–315, 2020.
- [10] J.-P. Chen, "Examinations concerning the electric discharge machining of AZ91/5B4CP composites utilizing distinctive electrode materials," *Materials and Manufacturing Processes*, vol. 34, no. 10, pp. 1120–1128, 2019.
- [11] M. Uthayakumar, K. V. Babu, S. T. Kumaran, S. S. Kumar, J. T. W. Jappes, and T. P. D. Rajan, "Study on the machining of Al-SiC functionally graded metal matrix composite using die-sinking EDM," *Particulate Science & Technology*, vol. 37, no. 1, pp. 103–109, 2019.
- [12] A. Torres, C. J. Luis, and I. Puertas, "Analysis of the influence of EDM parameters on surface finish, material removal rate, and electrode wear of an INCONEL 600 alloy," *International Journal of Advanced Manufacturing Technology*, vol. 80, no. 1, pp. 123–140, 2015.
- [13] Y.-C. Lin, C.-H. Cheng, B.-L. Su, and L.-R. Hwang, "Machining characteristics and optimization of machining parameters of SKH 57 high-speed steel using electrical-discharge machining based on Taguchi method," *Materials and Manufacturing Processes*, vol. 21, no. 8, pp. 922–929, 2006.
- [14] S. Raj and K. Kumar, "Optimization and prediction of material removing rate in die sinking electro discharge machining of EN45 steel tool," *Materials Today Proceedings*, vol. 2, no. 4-5, pp. 2346–2352, 2015.
- [15] T. Y. Saindane and H. G. Patil, "Optimization of various process parameter of EDM using Taguchi method with experimental validation," *International Journal of Engineering Sciences*, vol. 6, no. 3, pp. 2142–2146, 2016.
- [16] H. K. Kansal, S. Singh, and P. Kumar, "Technology and research developments in powder mixed electric discharge machining (PMEDM)," *Journal of Materials Processing Technology*, vol. 184, no. 1-3, pp. 32–41, 2007.
- [17] Y. Zhang, Y. Liu, Y. Shen et al., "A review of the current understanding and technology of powder mixed electrical discharge machining (PMEDM)," in *Proceedings of the 2012 IEEE International Conference on Mechatronics and Automation*, pp. 2240–2247, IEEE, Chengdu, China, August 2012.
- [18] M. P. Jahan, M. Rahman, and Y. S. Wong, "Modelling and experimental investigation on the effect of nanopowder-mixed dielectric in micro-electrodischarge machining of tungsten carbide," *Proceedings of the Institution of Mechanical*

- Engineers - Part B: Journal of Engineering Manufacture*, vol. 224, no. 11, pp. 1725–1739, 2010.
- [19] P. C. Tan and S. H. Yeo, "Investigation of recast layers generated by a powder-mixed dielectric micro electrical discharge machining process," *Proceedings of the Institution of Mechanical Engineers - Part B: Journal of Engineering Manufacture*, vol. 225, no. 7, pp. 1051–1062, 2011.
- [20] M. P. Jahan, M. Rahman, and Y. San Wong, "Study on the nano-powder-mixed sinking and milling micro-EDM of WC-Co," *International Journal of Advanced Manufacturing Technology*, vol. 53, no. 1-4, pp. 167–180, 2011.
- [21] S.-L. Chen, M.-H. Lin, G.-X. Huang, and C.-C. Wang, "Research of the recast layer on implant surface modified by micro-current electrical discharge machining using deionized water mixed with titanium powder as dielectric solvent," *Applied Surface Science*, vol. 311, pp. 47–53, 2014.
- [22] B. Kuriachen and J. Mathew, "Effect of powder mixed dielectric on material removal and surface modification in microelectric discharge machining of Ti-6Al-4V," *Materials and Manufacturing Processes*, vol. 31, no. 4, pp. 439–446, 2016.
- [23] R. Manivannan and M. P. Kumar, "Multi-attribute decision-making of cryogenically cooled micro-EDM drilling process parameters using TOPSIS method," *Materials and Manufacturing Processes*, vol. 32, no. 2, pp. 209–215, 2017.
- [24] C. Roy, K. H. Syed, and P. Kuppan, "Machinability of Al/10% SiC/2.5% TiB<sub>2</sub> metal matrix composite with powder-mixed electrical discharge machining," *Procedia Technology*, vol. 25, pp. 1056–1063, 2016.
- [25] G. Iyyapan, R. SudhakaraPandian, and M. Sakthivel, "Influence of silicon carbide mixed used engine oil dielectric fluid on EDM characteristics of AA7075/SiCp/B4Cp hybrid composites," *Materials Research Express*, vol. 8, 2021.
- [26] M. Prabhakar B S, R. R, and V. S, "Characterization of electric discharge machining of titanium alloy utilizing MEIOT technique for orthopedic implants," *Materials Research Express*, vol. 8, no. 8, Article ID 086505, 2021.
- [27] Y. Aboobucker Parvez and S. S. Abuthakeer, "Machining characteristics of Al<sub>2</sub>O<sub>3</sub> powder mixed electric discharge machining of aa7050/SiCp/Al<sub>2</sub>O<sub>3</sub>p hybrid composites," *ECS Journal of Solid State Science and Technology*, vol. 10, no. 7, Article ID 073007, 2021.
- [28] B. Xu, M. Q. Lian, S. G. Chen et al., "Combining PMEDM with the tool electrode sloshing to reduce recast layer of titanium alloy generated from EDM," *International Journal of Advanced Manufacturing Technology*, vol. 66, pp. 1–11, 2021.
- [29] S. Singh, B. Patel, R. K. Upadhyay, and N. K. Singh, "Improvement of process performance of powder mixed electrical discharge machining by optimisation -A Review," *Advances in Materials and Processing Technologies*, vol. 23, pp. 1–31, 2021.
- [30] C. Somu, R. Ranjith, G. Pytenkar, and M. Ramu, "A novel Cu-Gr composite electrode development for electric discharge machining of Inconel 718 alloy," *Surface Topography: Metrology and Properties*, vol. 32, 2021.
- [31] M. Bhaumik and K. Maity, "Effect of process parameters on the surface crack density of AISI 304 in PMEDM," *World Journal of Engineering*, vol. 51, 2017.
- [32] G. Singh, Y. Lamichhane, A. S. Bhui, S. S. Sidhu, P. S. Bains, and P. Mukhiya, "Surface morphology and microhardness behavior of 316L in hap-pmedm," *Facta Universitatis - Series: Mechanical Engineering*, vol. 17, no. 3, pp. 445–454, 2019.
- [33] P. K. Rout and P. C. Jena, "A review of current researches on powder mixed electrical discharge machining (PMEDM) technology," *Lecture Notes in Mechanical Engineering*, vol. 43, pp. 489–497, 2021.